Cross section of a magma conduit system at the margin of the Colorado Plateau

Keith Putirka* Department of Earth and Environmental Sciences, California State University, 2345 East San Ramon Avenue, MS MH24, Fresno, California 93740, USA
Christopher D. Condit* Geoscience Department, University of Massachusetts, Amherst, Massachusetts 01003-9297, USA

ABSTRACT

We present crystallization depth vs. temperature estimates for clinopyroxene phenocrysts from the Springerville volcanic field, Arizona. These calculations reveal several intriguing patterns that have considerable implications for magma transport and genesis. First, partial crystallization occurs over a wide depth range (0–60 km), but most partial crystallization occurs between 0 and 30 km. Second, low crystallization temperatures, low-density magmas, and evolved liquid compositions derive exclusively from two depth intervals, 0–12 and 23–30 km. These intervals coincide with a density contrast in the upper crust and a rheology contrast at the base of the middle crust. They also coincide with two highly seismically reflective depth intervals. These relationships indicate that (1) the Moho is not a staging area for volcanic eruptions; (2) density contrasts in the upper crust, and a rheology contrast in the middle crust, control magma transport and liquid evolution; (3) magma conduits are probably magma mush columns, with a preponderance of sills within the 0–12 and 23–30 km intervals; and (4) seismically reflective layers are sills related to Tertiary–Holocene volcanic activity. Moreover, these sills appear to represent the principal sites of magma evolution.

Keywords: magma chambers, petrology, magma contamination, seismic reflection profiles, barometry, geologic thermometry.

INTRODUCTION

Models of magma conduits commonly show the pooling and transport of magma at or from the base of the crust, where there is a significant density contrast (e.g., Hildreth and Moorbath, 1988; Yang et al., 1999). Although the Moho is the most commonly illustrated magma-staging region, petrologists also look to rheology contrasts (Gans et al., 1989; Parsons et al., 1992) and states of stress within the crust or lithosphere (Rubin and Pollard, 1987; Parsons and Thompson, 1993) as possible controls on magma transport. Additional models reject the concept of one or a few discrete magma chambers and instead argue for a plexus of dikes and sills (Ryan, 1988; Marsh, 1995). All such models carry implications regarding the depths at which phenocrysts crystallize. We test these models by calculating crystallization depths for clinopyroxene phenocrysts from the Springerville volcanic field, which is at the southern margin of the Colorado Plateau, in east-central Arizona.

We calculated crystallization pressures (*P*) and temperatures (*T*) (Putirka et al., 2003) for 32 eruptive units that span nearly the entire temporal range of magmatic activity at the Springerville volcanic field (8.7–0.3 Ma). The Springerville field is ideal for the application of igneous thermobarometers because the geology of the region is well known (Condit and Conner, 1996; Condit et al., 1999). In addition, geophysical and petrologic studies of the Colorado Plateau, and its transition zone with the Basin and Range Province, provide crucial information regarding the stratigraphy and structure of the crust (Parsons et al., 1996; Parsons et al., 1992; Condie and Selverstone, 1999). Such information allows us to compare crystallization depths to the physical quantities that nominally control magma mobility.

METHODS

P-T conditions were calculated (Putirka et al., 2003) using clinopyroxene–whole-rock pairs (Condit, 1995; http://ddm.geo.umass.edu/ddmsvfex/),[1] for which an approach to equilibrium was established (Fig. 1). An average of 7 points per clinopyroxene grain was averaged. The similarity of core and rim analyses indicates that most crystals are unzoned and homogeneous (Fig. 2A). No systematic compositional variations between phenocryst size and composition are apparent. Because whole-rock compositions might have been affected by olivine precipitation (Springerville lavas carry to 10 wt% olivine phenocrysts), mineral-melt equilibria are used to check that whole-rock compositions represent liquids. We use clinopyroxene and olivine Fe-Mg exchange coefficients: $K_D^{cpx\text{-}liq}$(Fe-Mg) = 0.27 (Putirka, 2003; $K_D^{cpx\text{-}liq}$(Fe-Mg) = [$MgO^{liq}FeO^{cpx}$]/[$MgO^{cpx}FeO^{liq}$]; MgO and FeO are cation fractions), and $K_D^{ol\text{-}liq}$(Fe-Mg) = 0.30 (Roeder and Emslie, 1970). Whole-rock compositions were adjusted to $K_D^{cpx\text{-}liq}$(Fe-Mg) = 0.27 by adding or subtracting olivine, which enforced an equilibrium value for $K_D^{cpx\text{-}liq}$(Fe-Mg).

As a further check on clinopyroxene-liquid equilibrium, we calculated equilibrium clinopyroxene compositions and *T* for clinopyroxene saturation using fractionation-adjusted whole rocks and calculated *P* as input (Putirka, 1999). Of the 149 clinopyroxenes analyzed, 122, from 20 eruptive units, yielded 3 characteristics that suggest an approach to equilibrium with their host rock. (1) Clinopyroxene component sums approach unity (Fig. 1A). (2) Calculated equilibrium components approach observed phenocryst compositions (Fig. 1A). (3) Clinopyroxene saturation and phenocryst temperatures (Putirka, 1999) match within 1σ model error (Fig. 1B). Moreover, *T* calculated from olivine phenocrysts (Putirka, 1997) matches *T* from clinopyroxene phenocrysts to within 1σ model error. Olivines yield somewhat higher *T* values (average = +37.5 °C) compared to clinopyroxenes (Fig. 1C), but this magnitude is consistent with adjustments for olivine fractionation, and probably reflects the early precipitation of olivine. We suggest that the relationships of Figure 1 are not coincidental, and that clinopyroxene *P-T* estimates are valid. Crystallization pressures (Fig. 2A) were converted to depths (Fig. 2B) using the density model of Condie and Selverstone (1999). Magma densities were calculated using the models of Lange and Carmichael (1990).

RESULTS

A plot of depth vs. *T* yields a cross section of the Springerville magma conduit system (Fig. 2B) with several notable features. First, phenocrysts are calculated to have crystallized over a wide depth range (0–58 km), but largely in the upper 30 km. Second, 11 eruptive units derived 90%–100% of their phenocrysts from either the 0–12 or the 23–30 interval (but not both; closed symbols in Fig. 2). Phenocrysts from remaining whole rocks yield less restricted depth ranges. In ad-

*E-mail: kputirka@csufresno.edu; ccondit@geo.umass.edu.

[1]GSA Data Repository item 2003099, whole-rock and clinopyroxene phenocryst analyses from the Springerville volcanic field, is available from Documents Secretary, GSA, P.O. Box 9140, Boulder, CO 80301-9140, editing@geosociety.org, or at www.geosociety.org/pubs/ft2003.htm.

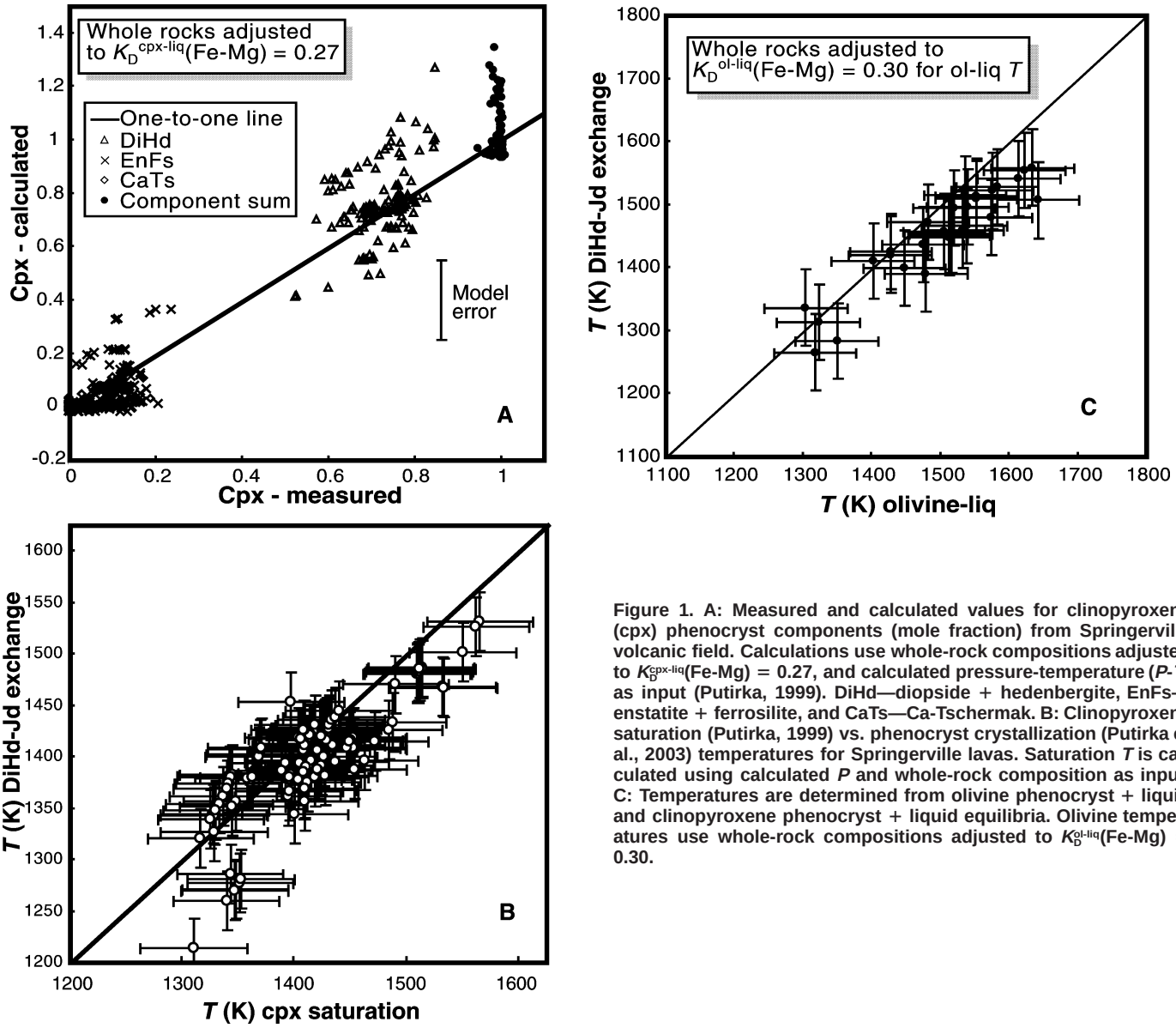

Figure 1. A: Measured and calculated values for clinopyroxene (cpx) phenocryst components (mole fraction) from Springerville volcanic field. Calculations use whole-rock compositions adjusted to $K_D^{cpx-liq}$(Fe-Mg) = 0.27, and calculated pressure-temperature (*P-T*) as input (Putirka, 1999). DiHd—diopside + hedenbergite, EnFs—enstatite + ferrosilite, and CaTs—Ca-Tschermak. B: Clinopyroxene saturation (Putirka, 1999) vs. phenocryst crystallization (Putirka et al., 2003) temperatures for Springerville lavas. Saturation *T* is calculated using calculated *P* and whole-rock composition as input. C: Temperatures are determined from olivine phenocryst + liquid and clinopyroxene phenocryst + liquid equilibria. Olivine temperatures use whole-rock compositions adjusted to K_D^{ol-liq}(Fe-Mg) = 0.30.

dition, low crystallization temperatures, evolved lava compositions, and low magma densities derive exclusively from the 0–12 and 23–30 km intervals (Figs. 2 and 3).

The depth intervals 0–12 and 23–30 km coincide with a density contrast in the upper crust and a rheology contrast in the middle crust (Fig. 2C) and exhibit a striking correspondence to seismically reflective layers of the Bagdad reflection sequence (0–12 km; Goodwin et al., 1989) and middle-crust high-amplitude seismic reflectors (21–29 km; Fig. 2C; Parsons et al., 1992). The Springerville volcanic field is ~200 km east of the seismic transects and is expected to have a similar crustal structure (T. Parsons, 2003, personal commun.).

DISCUSSION

Overall, the wide range of crystallization depths (Fig. 2) supports the concept of a magma mush column (Marsh, 1995). In addition, because evolved liquid compositions, low phenocryst temperatures, and anomalously low magma densities occur exclusively within the depth intervals 0–12 and 23–30 km, these intervals appear to be sites of prolonged magma storage.

To test for liquid evolution in these intervals, we compared K_2O, K/Ti, and SiO_2 of those lavas whose phenocrysts crystallized at either 0–12 or 23–30 km with those lavas whose phenocrysts crystallized at other depths. K/Ti is used because olivine and clinopyroxene are the only fractionating phases; K/Ti ratios are thus unlikely to be affected by fractional crystallization, but might be affected by crustal assimilation. It is significant that only those samples with elevated K_2O and K/Ti and $SiO_2 > 49$ wt% crystallized within the 0–12 and 23–30 km depth intervals. Moreover, K_2O, K/Ti, and SiO_2 are highly correlated with *T* for the 11 eruptive units that partially crystallized within these intervals (Fig. 3), but uncorrelated with *T* for the remaining lavas. K_2O concentrations suggest an important role for wall-rock assimilation. If we begin with the most primitive magma in Figure 3, and assume the best-case scenario that $D^{bulk}(K_2O) = 0$, 86% perfect fractional crystallization is required to obtain the observed range of K_2O. However, such crystal-rich products are unlikely to be erupted (Marsh, 1981). Elevated K_2O and K/Ti thus probably reflect assimilation of ambient crust.

What are the causes of magma stagnation? Staging depths of <12 km are consistent with a density control because incoming magmas are negatively buoyant within the upper crust (Fig. 2C). However, all Springerville magmas are less dense than the lower and middle crusts when uncompressed to such depths. A brittle-ductile transition could

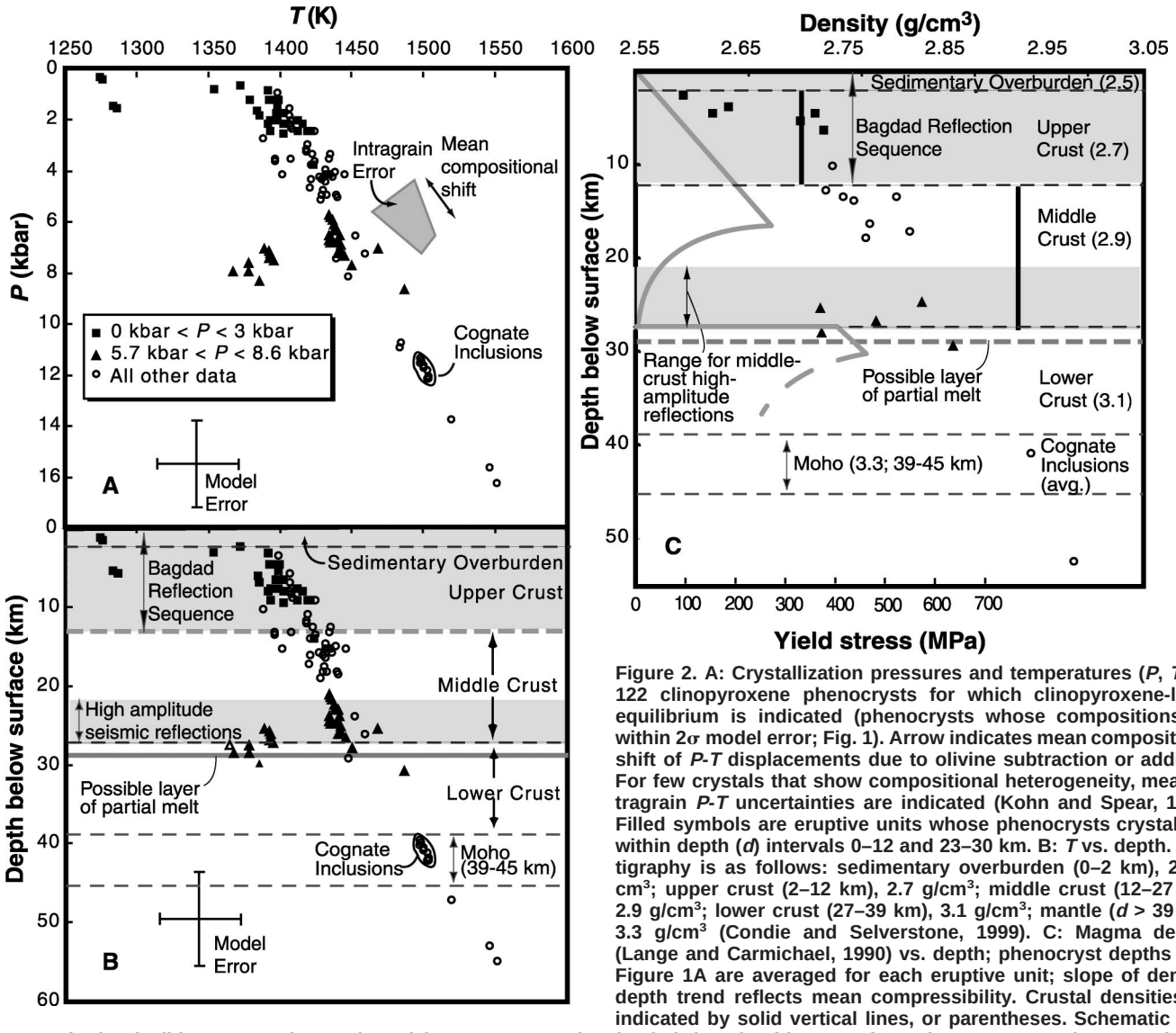

Figure 2. A: Crystallization pressures and temperatures (*P*, *T*) for 122 clinopyroxene phenocrysts for which clinopyroxene-liquid equilibrium is indicated (phenocrysts whose compositions are within 2σ model error; Fig. 1). Arrow indicates mean compositional shift of *P-T* displacements due to olivine subtraction or addition. For few crystals that show compositional heterogeneity, mean intragrain *P-T* uncertainties are indicated (Kohn and Spear, 1991). Filled symbols are eruptive units whose phenocrysts crystallized within depth (*d*) intervals 0–12 and 23–30 km. B: *T* vs. depth. Stratigraphy is as follows: sedimentary overburden (0–2 km), 2.5 g/cm^3; upper crust (2–12 km), 2.7 g/cm^3; middle crust (12–27 km), 2.9 g/cm^3; lower crust (27–39 km), 3.1 g/cm^3; mantle (*d* > 39 km), 3.3 g/cm^3 (Condie and Selverstone, 1999). C: Magma density (Lange and Carmichael, 1990) vs. depth; phenocryst depths from Figure 1A are averaged for each eruptive unit; slope of density-depth trend reflects mean compressibility. Crustal densities are indicated by solid vertical lines, or parentheses. Schematic yield stress magnitudes (solid gray curve) are adapted from Morgan and Golombek (1984), with strength maxima set to match compositional boundaries. Shaded regions indicate depth ranges for Bagdad reflection sequence and middle crust high-amplitude reflectors; dashed horizontal line at 29 km indicates depth to inferred zone of partial melt (Parsons et al., 1992); depths to reflectors are calculated assuming mean seismic velocity = 6.1 km/s (Condie and Selverstone, 1999).

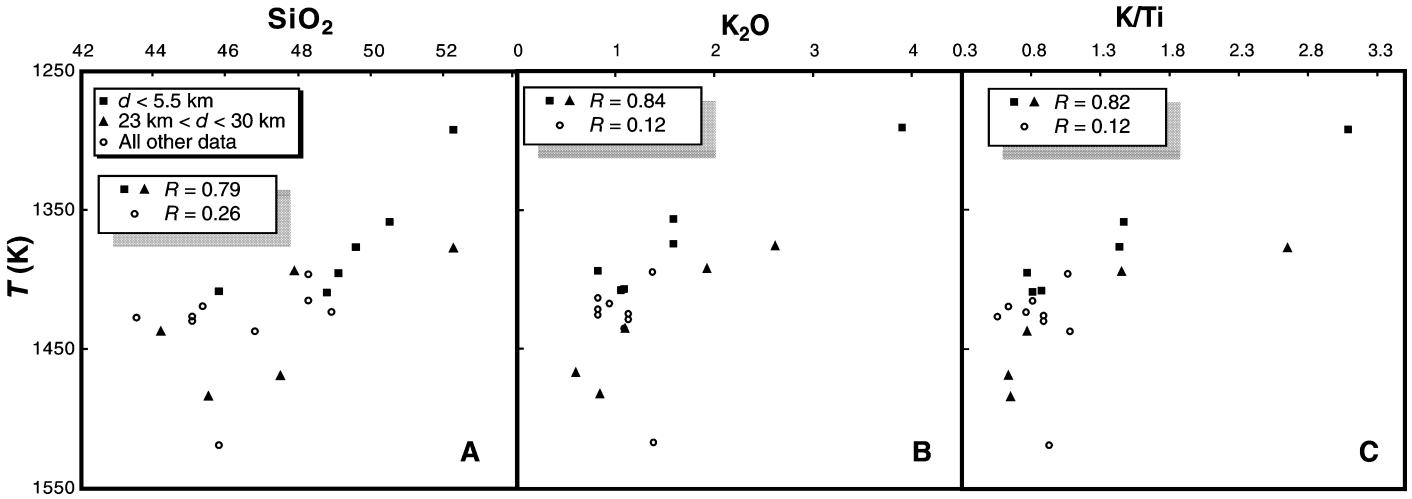

Figure 3. Mean crystallization temperature (*T*) vs. whole-rock composition: A: SiO_2. B: K_2O. C: K/Ti (mole fraction). Correlation coefficients, *R*, for eruptive units within and outside two stagnation depth (*d*) intervals are indicated (see Fig. 2A).

inhibit transport through fractures. For example, stress at a crack tip, σ, can be approximated by $\sigma = \sigma_r(1 + 2h/w) = \sigma_r(2h/\rho)^{0.5}$, where σ_r = remote stress, h = dike half-height, w = dike half-width, and ρ = radius of curvature at the fracture tip (Scholz, 1990); ρ should increase in a ductile region. Brittle-ductile transitions may occur at any depth >10 km (Carter and Tsenn, 1987), but are more likely to occur near compositional boundaries, such as between the middle and lower crust (Fig. 2C; Kruse et al., 1991; Morgan and Golombek, 1984). We thus agree with Parsons et al. (1992) that a rheology contrast is responsible for magma stagnation in the 23–30 km interval. Why do some magmas differentiate at such levels while some do not? Dike size might be a factor. Large dikes are more buoyant, and with high h/w will have greater stress intensities at their tips; they may thus more easily bypass potential magma traps. Given that dike velocity scales with σ, partial crystallization outside the 0–12 and 23–30 km intervals might also represent slowing of such dikes, rather than a complete stop.

What are the origins of the high reflectivity layers observed in seismic sections? Crystallization depths (Fig. 2) support the view that these layers are magmatic sills related to Tertiary–Holocene volcanic activity (Goodwin et al., 1989; Parsons et al. 1992). Geochemical relationships furthermore suggest that these sills are the primary sites of liquid evolution and wall-rock assimilation (Fig. 3).

SUMMARY

Crystallization depths from the Springerville volcanic field show that magmas partially crystallize and are erupted from a wide depth range, suggesting that the Springerville magma conduits comprise a magma mush column (Ryan, 1988; Marsh, 1995). Magmas appear to bypass the Moho without undergoing significant liquid evolution. Although crystallization occurs over a broad depth range, lavas with evolved compositions, low densities, and low crystallization temperatures contain phenocrysts that crystallized exclusively from two depth intervals, 0–12 and 23–30 km. Density and strength profiles suggest that these intervals coincide with a density and a rheology contrast, respectively. These intervals, however, are not barriers to all magmas—approximately half of Springerville magmas did not undergo significant partial crystallization at these contrasts, and we suspect that dike size is an important factor. Intervals of magmatic differentiation coincide with regional upper and middle crust seismic reflectors, suggesting that such reflectors represent Tertiary–Holocene magmatic sills (Parsons et al., 1992), and that these sills are the primary sites of liquid evolution.

ACKNOWLEDGMENTS

We thank Tony Morse and J. Michael Rhodes for their comments on an earlier draft of this manuscript, and Allen Glazner, Bruce Marsh, Tom Parsons, and an anonymous reader for helpful reviews.

REFERENCES CITED

Carter, N.L., and Tsenn, M.C., 1987, Flow properties of continental lithosphere: Tectonophysics, v. 136, p. 27–63.

Condie, K.C., and Selverstone, J., 1999, The crust of the Colorado Plateau: New views of an old arc: Journal of Geology, v. 107, p. 387–397.

Condit, C.D., 1995, Dynamic digital map: The Springerville Volcanic Field: Prototype color digital maps with ancillary data: Geological Society of America Digital Publication Series DPSM01MC, version 4.10.95.

Condit, C.D., and Conner, C.B., 1996, Recurrence rates of volcanism in basaltic volcanic fields; an example from the Springerville volcanic field, Arizona: Geological Society of America Bulletin, v. 108, p. 1225–1241.

Condit, C.D., Crumpler, L.S., and Aubele, J.C., 1999, Lithologic, age group, magnetopolarity, and geochemical maps of the Springerville volcanic field, east-central Arizona: U.S. Geological Survey Miscellaneous Investigations Map I-2431, scale 1:100,000.

Gans, P.B., Mahood, G.A., and Schermer, E., 1989, Synextensional magmatism in the Basin and Range Province: Geological Society of America Special Paper 233, 53 p.

Goodwin, E.B., Thompson, G.A., and Okaya, D.A., 1989, Seismic identification of basement reflectors: The Bagdad reflection sequence in the Basin and Range Province–Colorado Plateau transition zone, Arizona: Tectonics, v. 8, p. 821–831.

Hildreth, W., and Moorbath, S., 1988, Crustal contributions to arc magmatism in the Andes of central Chile: Contributions to Mineralogy and Petrology, v. 98, p. 455–489.

Kohn, M.T., and Spear, F.J., 1991, Error propagation for barometers: 2. Applications to rocks: American Mineralogist, v. 76, p. 138–147.

Kruse, S., McNutt, M., Phipps-Morgan, J., and Roydan, L., 1991, Lithospheric extension near Lake Mead, Nevada: A model for ductile flow in the lower crust: Journal of Geophysical Research, v. 96, p. 4435–4456.

Lange, R.L., and Carmichael, I.S.E., 1990, Thermodynamic properties of silicate liquids with emphasis on density, thermal expansion and compressibility, *in* Nicholls, J., and Russell, J.K., eds., Modern methods of igneous petrology: American Mineralogical Society Reviews in Mineralogy, v. 24, p. 25–64.

Marsh, B.D., 1981, On the crystallinity, probability of occurrence and rheology of lava and magma: Contributions to Mineralogy and Petrology, v. 78, p. 85–98.

Marsh, B.D., 1995, Solidification fronts and magmatic evolution: Mineralogical Magazine, v. 60, p. 5–40.

Morgan, P., and Golombek, M.P., 1984, Factors controlling the phases and styles of extension in the northern Rio Grande Rift: New Mexico Geological Society Field Conference Guidebook, v. 35, p. 13–19.

Parsons, T., and Thompson, G.A., 1993, Does magmatism influence low-angle normal faulting?: Geology, v. 21, p. 247–250.

Parsons, T., Howie, J.M., and Thompson, G.A., 1992, Seismic constraints on the nature of the lower crustal reflectors beneath the extending southern transition zone of the Colorado Plateau, Arizona: Journal of Geophysical Research, v. 97, p. 12,391–12,407.

Parsons, T., McCarthy, J., Kohler, W.M., Ammon, C.J., Benz, H.M., Hole, J.A., and Criley, E.E., 1996, Crustal structure of the Colorado Plateau, Arizona: Application of new long-offset seismic data analysis techniques: Journal of Geophysical Research, v. 101, p. 11,173–11,194.

Putirka, K., 1997, Magma transport at Hawaii: Inferences based on igneous thermobarometry: Geology, v. 25, p. 69–72.

Putirka, K., 1999, Clinopyroxene + liquid equilibria to 100 kbar and 2450 K: Contributions to Mineralogy and Petrology, v. 135, p. 151–163.

Putirka, K., Mikaelian, H., Ryerson, F., and Shaw, H., 2003, New clinopyroxene-liquid thermobarometers for mafic, evolved and volatile-bearing lava compositions, with applications to lavas from Tibet and the Snake River Plain, ID: American Mineralogist (in press).

Roeder, P.L., and Emslie, R.F., 1970, Olivine-liquid equilibrium: Contributions to Mineralogy and Petrology, v. 29, p. 275–289.

Rubin, A.M., and Pollard, D.D., 1987, Origins of blade-like dikes in volcanic rift zones: U.S. Geological Survey Professional Paper 1350, p. 1449–1470.

Ryan, M.P., 1988, The mechanics and three-dimensional internal structure of active magmatic systems: Kilauea volcano, Hawaii: Journal of Geophysical Research, v. 93, p. 4213–4248.

Scholz, C., 1990, The mechanics of earthquakes and faulting: Cambridge, Cambridge University Press, 439 p.

Yang, H.-J., Frey, F.A., Clague, D.A., and Garcia, M.O., 1999, Mineral chemistry of submarine lavas from Hilo Ridge, Hawaii; implications for magmatic processes within Hawaiian rift zones: Contributions to Mineralogy and Petrology, v. 135, p. 355–372.

Manuscript received 29 January 2003
Revised manuscript received 25 April 2003
Manuscript accepted 30 April 2003

Printed in USA